Determination of long non-coding RNAs associated with EZH2 in neuroblastoma by RIP-seq, RNA-seq and ChIP-seq

MUJIE YE[1,2*], LULU XIE[1,2*], JINGJING ZHANG[3*], BAIHUI LIU[1,2], XIANGQI LIU[1,2], JIAJUN HE[1,2], DUAN MA[4,5] and KUIRAN DONG[1,2]

[1]Department of Pediatric Surgery, Children's Hospital of Fudan University; [2]Key Laboratory of Neonatal Disease, Ministry of Health, Shanghai 201102; [3]Department of Medical Imaging, Nanjing Hospital of Chinese Medicine Affiliated to Nanjing University of Chinese Medicine, Nanjing, Jiangsu 210001; [4]Key Laboratory of Metabolism and Molecular Medicine, Ministry of Education, Department of Biochemistry and Molecular Biology, Institute of Biomedical Sciences, Collaborative Innovation Center of Genetics and Development, School of Basic Medical Sciences, Fudan University; [5]Shanghai Key Lab of Birth Defect, Children's Hospital of Fudan University, Shanghai 200032, P.R. China

Received August 3, 2019; Accepted May 22, 2020

DOI: 10.3892/ol.2020.11862

Abstract. Neuroblastoma (NB) is the most common type of extracranial solid tumor found in children. Despite several treatment options, patients with advanced stage disease have a poor prognosis. Previous studies have reported that enhancer of zeste homolog 2 (EZH2) and long non-coding RNAs (lncRNAs) have abnormal expression levels in NB and participate in tumorigenesis and NB development. However, the association between EZH2 and lncRNAs remain unclear. In the present study, RNA immunoprecipitation-sequencing (RIP-seq) was used to analyze the lncRNAs binding to EZH2. Following EZH2 knockdown via short hairpin RNA, RNA-seq was performed in shEZH2 and control groups in SH-SY5Y cells. Chromatin IP (ChIP)-seq was used to determine the genes that may be regulated by EZH2. Gene Ontology and Kyoto Encyclopedia of Genes and Genomes analyses were performed to identify the signaling pathways involved in NB. The results from RIP-seq identified 94 lncRNAs, including SNHG7, SNHG22, KTN-AS1 and Linc00843. Furthermore, results from RNA-seq demonstrated that, following EZH2 knockdown, 448 genes were up- and 571 genes were downregulated, with 32 lncRNAs up- and 35 downregulated and differentially expressed compared with control groups. Certain lncRNAs, including MALAT1, H19, Linc01021 and SNHG5, were differentially expressed in EZH2-knockdown group compared with the control group. ChIP-seq identified EZH2 located in the promoter region of 138 lncRNAs including CASC16, CASC15, LINC00694 and TBX5-AS1. In summary, the present study demonstrated that certain lncRNAs directly bound EZH2 and regulated EZH2 expression levels. A number of these lncRNAs that are associated with EZH2 may participate in NB tumorigenesis.

Correspondence to: Professor Kuiran Dong, Department of Pediatric Surgery, Children's Hospital of Fudan University, 399 Wanyuan Road, Minhang, Shanghai 201102, P.R. China
E-mail: kuirand@hotmail.com

Professor Duan Ma, Key Laboratory of Metabolism and Molecular Medicine, Ministry of Education, Department of Biochemistry and Molecular Biology, Institute of Biomedical Sciences, Collaborative Innovation Center of Genetics and Development, School of Basic Medical Sciences, Fudan University, 130 Dongan Road, Xuhui, Shanghai 200032, P.R. China
E-mail: duanma@fudan.edu.cn

*Contributed equally

Abbreviations: PRC2, polycomb repressor complex 2; RNA-seq, RNA sequencing; RIP-seq, RNA immunoprecipitation sequencing; ChIP-seq, chromatin immunoprecipitation sequencing; GO, Gene Ontology; KEGG, Kyoto Encyclopedia of Genes and Genomes

Key words: long non-coding RNA, neuroblastoma, enhancer of zeste homolog 2, sequence, signaling pathway

Introduction

Neuroblastoma (NB) is an embryonic tumor derived from sympathetic neural crest cells (1,2). It is the most common type of extracranial solid tumor found in children and the most common type of malignant tumor found in infants and young children, with an incidence rate of 10.5 per million children younger than 14 years old (3-5). The site of the disease is concealed, and NB easily metastasizes (5). Low-risk NB has the characteristics of regression and inducing NB differentiation and maturation *in vitro*, while high-risk NB has high malignancy and can metastasize early (6). The prognosis of patients with NB is extremely poor, which accounts for ~12-15% of all pediatric cancer-associated deaths (7,8). In recent years, treatments for low- and medium-risk NB have improved; however, the cure rate for patients with high-risk

NB remains low (9,10). It is therefore crucial to develop novel treatments for patients with high-risk NB.

Enhancer of zeste homolog 2 (EZH2) protein is the core catalytic element of polycomb repressor complex 2 (PRC2), which regulates the transcription of target genes via promoting histone H3 methylation (11-13). Previous studies have demonstrated that high expression level of EZH2 is a poor prognostic factor in various types of cancer (14,15). For example, in pancreatic cancer, EZH2-mediated microRNA-139-5p regulates epithelial-mesenchymal transition and lymph node metastasis (16). Moreover, EZH2 and EED directly regulate androgen receptor in advanced prostate cancer (17). In NB, EZH2 is highly expressed and can epigenetically silences NB tumor suppressor genes, including CASZ1, CLU, RUNX3 and NGFR, suggesting that EZH2 may be an NB molecular target (18).

Long non-coding RNAs (lncRNAs) are a type of RNA of >200 nucleotides in length that do not encode for proteins. Following their discovery, lncRNAs were considered as 'noises' in the genome transcription process (19,20). However, subsequent studies demonstrated that lncRNAs regulate genes at a number of levels, including epigenetic, genomic transcription and post-transcriptional levels. lncRNAs participate in cancer development and tumorigenesis by affecting tumor cell proliferation, migration, invasion, apoptosis and the cell cycle, and promoting angiogenesis (21,22). lncRNAs directly bind to EZH2, recruiting it to the promoter region of genes to repress their expression levels. lncRNAs also serve as EZH2 effectors or regulators (23-25). The present study investigated the association between lncRNAs and EZH2 using RNA immunoprecipitation (RIP)-, RNA- and chromatin IP-sequencing (ChIP-seq).

Materials and methods

Cell culture. The SH-SY5Y cell line was obtained from the American Type Culture Collection (cat. no. CRL-2266) and the 293T cell line was obtained from the Cell Bank of Type Culture Collection of the Chinese Academy of Sciences. Cells were cultured in Dulbecco's Modified Eagle Medium supplemented with 10% FBS and 1% penicillin-streptomycin solution (all from Biological Industries) and placed in a humidified incubator with 5% CO_2 at 37˚C. Cell culture dishes were obtained from Hangzhou Xinyou Biotechnology Co., Ltd.

Construction of short hairpin (sh)RNAs and stable transfected cell lines. EZH2 shRNA plasmids [designed online (http//www.sigmaaldrich.com)] and pLKO1(Genomeditech, Shanghai, China) were selected as vectors. The shRNA target sequences were as follows: Forward shEZH2-F, 5'-CCGGCCCAACATAGATGGACCAAATCTCGAGATTTGGTCCATCTATGTTGGGTTTTTG-3'; reverse shEZH2-R, 5'AATTCAAAAACCCAACATAGATGGACCAAATCTCGAGATTTGGTCCATCTATGTTGGG-3'; forward shControl-F, 5'-CCGGTTCTCCGAACGTGTCACGTCTCGAGACGTGACACGTTCGGAGAATTTTTG-3'; reverse shControl-R, 5'-AATTCAAAAAATTCTCCGAACGTGTCACGTCTCGAGACGTGACACGTTCGGAGAA. Lentivirus with shEZH2 was packaged with 293T cells using transfection reagent Lipofectamine® 2000 (Invitrogen; Thermo Fisher Scientific, Inc.). Stably transfected SH-SY5Y cells with shRNA (12 μg) and control (12 μg) were acquired following puromycin selection.

Western blotting. Cell were lysed using RIPA lysis buffer (Beyotime Institute of Biotechnology) on ice, and western blotting was performed as standard (26). Following blocking with 8% skimmed milk for 1 h at room temperature, membranes were incubated with primary antibodies (EZH2; cat. no. 5246S; and β-tubulin; cat. no. 2146S; Cell Signaling Technology, Inc.) on a decolorization shaker at 4˚C overnight. After washing with Tris-HCl + 0.05% Tween-20 TBST three times, membranes were incubated with secondary antibody (goat anti-rabbit IgG; 1:2,000; cat. no. CW0107; CoWin Biosciences) for 1 h at room temperature. Protein signals were detected via enhanced chemiluminescence substrate (EMD Millipore).

RIP-seq. RNA Immunoprecipitation (RIP) was performed followed as Gagliardi *et al* (27) In simple terms, RNA was enriched with EZH2 antibody (1:100; cat. no. 5246S; Cell Signaling Technology, Inc) in SH-SY5Y cells. Enriched RNA was broken into short fragments using fragmentation buffer (cat. no. N402-VAHTS; Vazyme Biotech Co., Ltd.) at 94˚C for 5 min. Fragmented mRNA was used as a template to synthesize cDNA using random hexamers, buffer, dNTPs and DNA polymerase I (VAHTS Stranded mRNA-seq Library Prep kit for Illumina; cat. no. NR602-01; Vazyme Biotech Co., Ltd.). After the synthesis of the double-stranded cDNA, the double-stranded cDNA was purified. LC magnetic beads were used for purification and target fragment binding. The EP tube was placed on a magnetic stand (beads combined with cDNA), then the supernatant was removed, and washed twice with 80% ethanol for 30 sec each time. End-repair and library preparation was performed by the aforementioned kit (VAHTS Stranded mRNA-seq Library Prep kit for Illumina). Target size selection was performed together with magnetic purification. PCR amplification (using Amplification Mix; cat. no. N611-01; Vazyme Biotech Co., Ltd.) was then performed as following: Initial denaturation 95˚C for 3 min, 12 cycles of denaturation at 98˚C for 20 sec, annealing at 55˚C for 15 sec, elongation at 72˚C for 30 sec, and final extension 72˚C for 5 min. The primer sequences of PCR were as follows: Forward, 5'AATGATACGGCGACCACCGAGATCTACACACACTCTTTCCCTACACGACGCTCTTCCGATCT-3'; reverse, 5'-CAAGCAGAAGACGGCATACGAGATGTGACTGGAGTTCAGACGTGTGCTCTTCCGATCT-3'. Agarose electrophoresis was used for quality inspection of the constructed library. Qubit 2.0 (Invitrogen; Thermo Fisher Scientific, Inc.) was used to detect the concentration of the library, and the loading concentration of the library was 42 ng/μl with 20 μl. After library quality tests were passed, libraries were sequenced using an Novaseq 6000 sequencer (Illumina, Inc.) with PE150 model (double-ended 150 bp sequencing) according to effective concentration and target data volume. RIP-seq and subsequent bioinformatics Gene Ontology (GO) and Kyoto Encyclopedia of Genes and Genomes (KEGG) analysis was performed by Hangzhou Lianchuan Biotechnology Co., Ltd with the DAVID website (https://david.ncifcrf.gov/).

RNA-seq and analysis. EZH2 protein was knocked down in SH-SY5Y cells using shRNA. Total RNA was obtained from

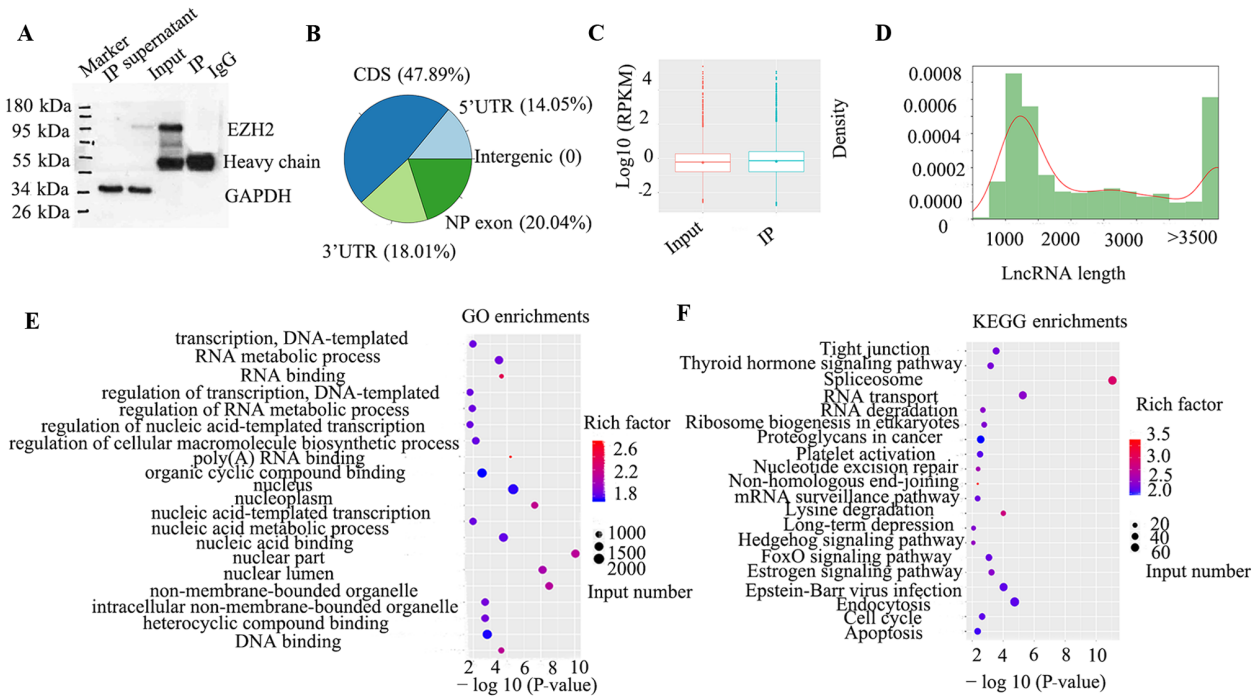

Figure 1. RNA IP-sequencing for lncRNAs binding with EZH2. (A) Western blotting of EZH2 immunoprecipitation. (B) Distribution statistics of peaks in each functional area of gene. NP exon is the exon region of the non-coding gene. (C) All gene RPKM profiles for characteristics of gene expression levels of the sample. (D) Length distribution statistics for known lncRNAs. (E) Gene Ontology and (F) Kyoto Encyclopedia of Genes and Genomes metabolic pathway enrichment analysis of peak-associated genes. Horizontal axis represents significance of enrichment [$-\log_{10}$ (P-value)], with larger values indicating more significant enrichment. Vertical axis represents enriched terms. Dot size indicates number of differential genes in terms, and dot color indicates the degree of rich factor enrichment. Most significant top 20 terms were selected by sorting by P-value. IP, immunoprecipitation; lncRNA, long non-coding RNA; EZH2, enhancer of zeste homolog 2; UTR, untranslated region; CDS, coding region; NP, no protein.

EZH2 knockdown and control groups with TRIzol® (Takara Bio, Inc.). Each group included three replicates. Illumina Paired End Sample Prep kits (Illumina, Inc.) were used to prepare libraries. Each cDNA library was sequenced using an Illumina Hiseq 4000 (cat. no. PE150; Illumina, Inc.). Differential expression levels of lncRNA and mRNA transcripts between the EZH2 knockdown and control groups were measured. RNA-seq and subsequent GO and KEGG analysis was performed by Hangzhou Lianchuan Biotechnology Co., Ltd following the previous study (28).

ChIP-seq. Cells from one 10-cm dish of 80-90% confluence cultures were sonicated 4 times for (30 sec on and 30 sec off) in precooled conditions (Fisher Sonic Dismembrator; Thermo Fisher Scientific, Inc.). DNA was disrupted into fragments of 200-1,000 bp by nucleic acid gel. Anti-EZH2 (1:100; cat. no. 5246S; Cell Signaling Technology, Inc) was used to capture chromatin fragments from cell extracts, and libraries were constructed from immunoprecipitated DNA. An Illumina sequencer was used for high-throughput sequencing of lncRNA and mRNA. ChIP-seq and subsequent GO and KEGG analysis were performed by Hangzhou Lianchuan Biotechnology Co., Ltd. The ChIP protocol was conducted as previously described by Kong *et al* (29).

Differential expression level analysis. Gene expression levels were estimated using fragments per kilobase of transcript per million mapped reads (FPKM) values. Cuffdiff (v2.1.1; http://cole-trapnell-lab.github.io/cufflinks/) was used to calculate FPKM values of lncRNAs and mRNAs.DAVID (https://david.ncifcrf.gov/) was used to perform GO and KEGG analysis. Official gene symbols of the significantly different genes were enriched. We followed the instructions on the website step by step until acquiring GO and KEGG terms. Significantly differentially expressed genes were obtained using P-value <0.05.

Results

RIP-seq identifies EZH2-interacting lncRNAs. RNA Immunoprecipitation (RIP) was performed using SH-SY5Y cells and western blotting was used to check IP efficiency (Fig. 1A). Both IP supernatants and inputs showed bands for the internal reference gene GAPDH, demonstrating protein extraction and the western blotting system is successful. Antibody heavy chain was detected in the IP and IgG lanes, indicating that IP was successful. Distribution statistics for peaks of each functional area of the gene demonstrated that the coding region accounted for 50% and the exon region of a non-coding gene was ~20% (Fig. 1B). By analyzing the distribution of RPKM values, the gene expression level characteristics of the sample were treated as a whole. If IP was significantly enriched compared with the input group, the total expression level of all genes in the IP group should have been higher than that in the input group (Fig. 1C). lncRNAs are >200 nucleotides in length. Length distribution statistics of known lncRNAs were determined. The results demonstrated that lncRNAs 500-1,000 and >3,500 bp in length were significantly more common than lncRNAs of other lengths

Table I. lncRNAs determined by RNA immunoprecipitation-sequencing.

lncRNA name	lncRNA ID	lncRNA type	Chromosome
AF001548.2-201	ENST00000574212	antisense_RNA	16
AC087280.2-201	ENST00000637205	lincRNA	11
HOXA11-AS-205	ENST00000522863	antisense_RNA	7
PCBP1-AS1-210	ENST00000416395	antisense_RNA	2
AP002383.3-201	ENST00000545958	antisense_RNA	11
CCDC18-AS1-205	ENST00000421202	lincRNA	1
AL096701.3-202	ENST00000483736	antisense_RNA	22
AC020661.4-201	ENST00000561388	antisense_RNA	15
PITRM1-AS1-201	ENST00000430356	antisense_RNA	10
AL121759.1-201	ENST00000434043	antisense_RNA	20
AC244517.2-201	ENST00000607216	antisense_RNA	5
PPP1R26-AS1-202	ENST00000603624	antisense_RNA	9
AC025188.1-201	ENST00000507514	antisense_RNA	5
AC092115.3-201	ENST00000575838	antisense_RNA	16
RAB11B-AS1-201	ENST00000593581	antisense_RNA	19
AC069503.1-201	ENST00000538710	lincRNA	12
LINC00843-201	ENST00000429104	lincRNA	10
AC011477.3-201	ENST00000585571	antisense_RNA	19
AC010320.4-201	ENST00000594379	antisense_RNA	19
AL135787.1-201	ENST00000450154	antisense_RNA	9
AC109587.1-201	ENST00000482368	antisense_RNA	3
FAM201A-201	ENST00000377680	antisense_RNA	9
SNHG7-201	ENST00000414282	antisense_RNA	9
AC138150.1-201	ENST00000589950	antisense_RNA	17
EMX2OS-206	ENST00000551288	antisense_RNA	10
AC137932.1-201	ENST00000563087	antisense_RNA	16
AC005920.2-201	ENST00000509833	antisense_RNA	17
MZF1-AS1-202	ENST00000600534	antisense_RNA	19
AC080112.2-201	ENST00000578774	antisense_RNA	17
AC008741.1-201	ENST00000569456	antisense_RNA	16
AC024563.1-201	ENST00000601860	antisense_RNA	19
AC020911.1-201	ENST00000591038	antisense_RNA	19
AC097467.3-216	ENST00000599555	antisense_RNA	4
C5orf66-205	ENST00000555438	antisense_RNA	5
SGO1-AS1-204	ENST00000634618	lincRNA	3
AC011603.3-201	ENST00000549516	antisense_RNA	12
ADIRF-AS1-203	ENST00000609111	antisense_RNA	10
AC106864.1-201	ENST00000510655	antisense_RNA	4
AC093110.1-202	ENST00000626206	antisense_RNA	2
MCM3AP-AS1-201	ENST00000414659	antisense_RNA	21
AC108449.1-202	ENST00000517632	antisense_RNA	8
AC004923.4-201	ENST00000532296	antisense_RNA	11
KDM4A-AS1-203	ENST00000434346	antisense_RNA	1
FO393401.1-201	ENST00000453914	antisense_RNA	20
AC078777.1-201	ENST00000425371	antisense_RNA	12
PDZRN3-AS1-201	ENST00000478988	antisense_RNA	3
AL139423.1-201	ENST00000606802	antisense_RNA	1
AL118558.1-201	ENST00000557551	antisense_RNA	14
FOXD1-AS1-201	ENST00000514661	lincRNA	5
ZFPM2-AS1-207	ENST00000524045	antisense_RNA	8
AC073167.1-201	ENST00000559303	antisense_RNA	15
SH3BP5-AS1-202	ENST00000420195	antisense_RNA	3

Table I. Continued.

lncRNA name	lncRNA ID	lncRNA type	Chromosome
AC012170.2-201	ENST00000560380	antisense_RNA	15
NEXN-AS1-201	ENST00000421331	antisense_RNA	1
AC092329.1-201	ENST00000594653	lincRNA	19
DNMBP-AS1-202	ENST00000434409	antisense_RNA	10
AC013391.1-201	ENST00000560477	antisense_RNA	15
PKP4-AS1-201	ENST00000342892	antisense_RNA	2
LINC01089-202	ENST00000429892	lincRNA	12
AC010978.1-202	ENST00000427050	antisense_RNA	2
AL606534.3-201	ENST00000437499	antisense_RNA	1
AL606534.1-201	ENST00000439562	antisense_RNA	1
AL356599.1-205	ENST00000606388	antisense_RNA	6
KTN1-AS1-202	ENST00000412224	antisense_RNA	14
AC004893.2-201	ENST00000360902	antisense_RNA	7
AC087286.3-201	ENST00000561409	antisense_RNA	15
AL139021.2-201	ENST00000556390	antisense_RNA	14
C1orf220-202	ENST00000521244	lincRNA	1
H1FX-AS1-201	ENST00000383461	antisense_RNA	3
SEC62-AS1-201	ENST00000479626	antisense_RNA	3
AL161747.2-201	ENST00000535893	antisense_RNA	14
DDN-AS1-202	ENST00000547866	antisense_RNA	12
TTC3-AS1-201	ENST00000424733	antisense_RNA	1
AC245452.1-201	ENST00000458178	antisense_RNA	22
AC008676.1-201	ENST00000508443	antisense_RNA	5
AC022395.1-201	ENST00000451610	antisense_RNA	10
AC010976.1-203	ENST00000629005	antisense_RNA	2
AP000229.1-201	ENST00000608591	lincRNA	21
AC026427.1-201	ENST00000508993	antisense_RNA	5
AC025043.1-201	ENST00000558047	antisense_RNA	15
SLC16A1-AS1-204	ENST00000428411	antisense_RNA	1
ZNF337-AS1-201	ENST00000414393	antisense_RNA	20
AL451047.1-201	ENST00000424451	antisense_RNA	1
AC009185.1-201	ENST00000517634	antisense_RNA	5
AC023790.2-201	ENST00000543321	lincRNA	12
AC092143.3-201	ENST00000565150	antisense_RNA	16
ASH1L-AS1-202	ENST00000456633	antisense_RNA	1
SPG20-AS1-203	ENST00000493739	antisense_RNA	13
ALKBH3-AS1-201	ENST00000499194	antisense_RNA	11
SNHG22-201	ENST00000589499	antisense_RNA	18
AC010624.3-201	ENST00000599914	antisense_RNA	19
AL592166.1-202	ENST00000428791	antisense_RNA	1

lncRNA, long non-coding RNA; lincRNA, large intergenic noncoding RNA.

in SH-SY5Y cells (Fig. 1D). A total of 2,595 lncRNAs were identified by counting peaks associated with known lncRNAs. Among these lncRNAs, 94 were identified via exclusion of processed transcripts and retained introns (Table I). GO analysis demonstrated that these lncRNAs were involved in numerous biological processes, including cellular components and molecular functions, such as metabolic process and transcription regulation(Fig. 1E). Furthermore, KEGG analysis indicated that 'Hedgehog signaling pathway' and 'FoxO signaling pathway' were enriched in SH-SY5Y cells. 'Tight junction', 'apoptosis' and 'cell cycle' may also be associated with these lncRNAs (Fig. 1F).

RNA-seq for mRNAs and lncRNAs. The results from western blotting demonstrated that EZH2 was significantly downregulated following shRNA transfection (Fig. 2A). By analyzing

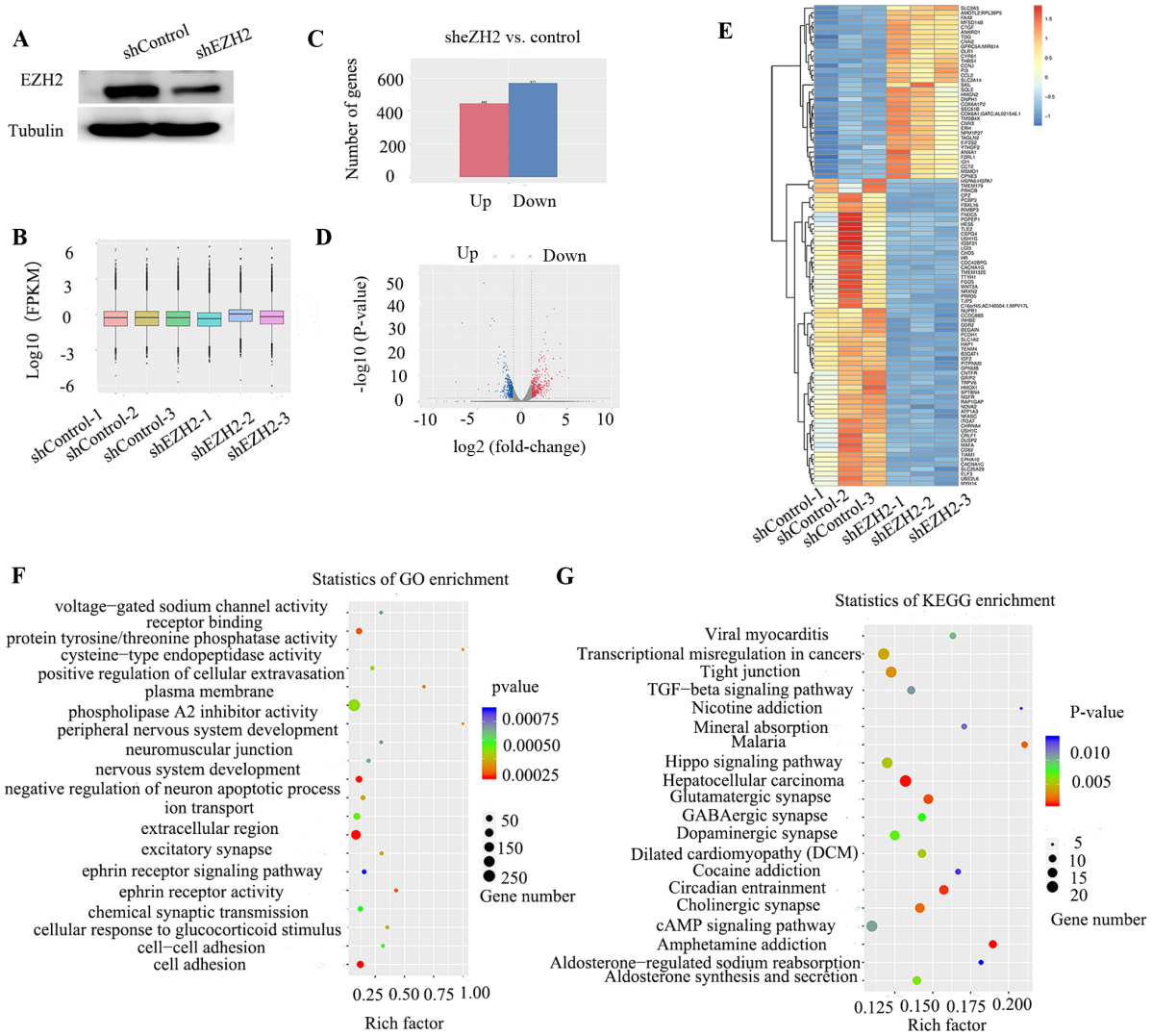

Figure 2. RNA-sequencing for differentially expressed mRNAs. (A) Western blotting of EZH2 knockdown efficiency. (B) Boxplot of FPKM profiles of all genes. (C) Bar and (D) volcano plots and (E) heatmap of differentially expressed genes for shEZH2 vs. shControl. (F) GO and (G) Kyoto Encyclopedia of Genes and Genomes metabolic pathway enrichment analysis of peak-associated genes. EZH2, enhancer of zeste homolog 2; FPKM, fragments per kilobase of transcript per million mapped reads; sh, short hairpin; GO, Gene Ontology.

the distribution of FPKM values, the gene expression level characteristics of the sample were treated as a whole (Fig. 2B). Following EZH2 knockdown, 448 up- and 571 downregulated genes were differentially expressed compared with the normal control group (Fig. 2C and D). A heatmap of the top 100 differentially expressed genes was generated (Fig. 2E). GO analysis demonstrated that these genes were associated with 'negative regulation of neuron apoptotic processes', 'nervous system development' and 'peripheral nervous system development'. KEGG analysis showed that enriched genes were primarily distributed in the 'TGF-β signaling pathway', 'Hippo signaling pathway' and 'cAMP signaling pathway'. Compared with the normal control group, 32 up- and 35 downregulated lncRNAs were differentially expressed in the shEZH2 group (Fig. 3A and B; Table II). A heatmap of the top 100 differentially expressed lncRNAs (including known and novel lncRNAs) was generated (Fig. 3C). GO analysis demonstrated that these lncRNAs were involved in numerous biological processes, including 'regulation of developmental growth', 'peptidyl-tyrosine phosphorylation' and 'histone glutamine methylation' (Fig. 3D). KEGG analysis demonstrated that 'Hedgehog signaling pathway', 'Parkinson's disease' and 'Alzheimer's disease' were associated with these lncRNAs (Fig. 3E).

ChIP-seq for EZH2. Due to the influence of chromosome conformation, chromosome expression levels in the active region of gene expression levels was more open. This resulted in input DNA reads exhibiting greater abundance in promoter and gene body regions, with a characteristic decrease near the transcription start site (TSS). The distribution of IP DNA is associated with EZH2 proteins, and apparent modifications such as transcription factors and H3K27me3 were enriched in the promoter and gene body regions. Through the distribution of reads in the intervals of these genes, the success of ChIP-seq experiments was verified (Fig. 4B). Analysis of peak distribution in the genomic functional area indicated that intergenic and promoter-TSS were the most frequent areas (Fig. 4A). ChIP-seq identified 634 genes located in the promoter region, including 138 long intervening non-coding RNAs (lincRNA;

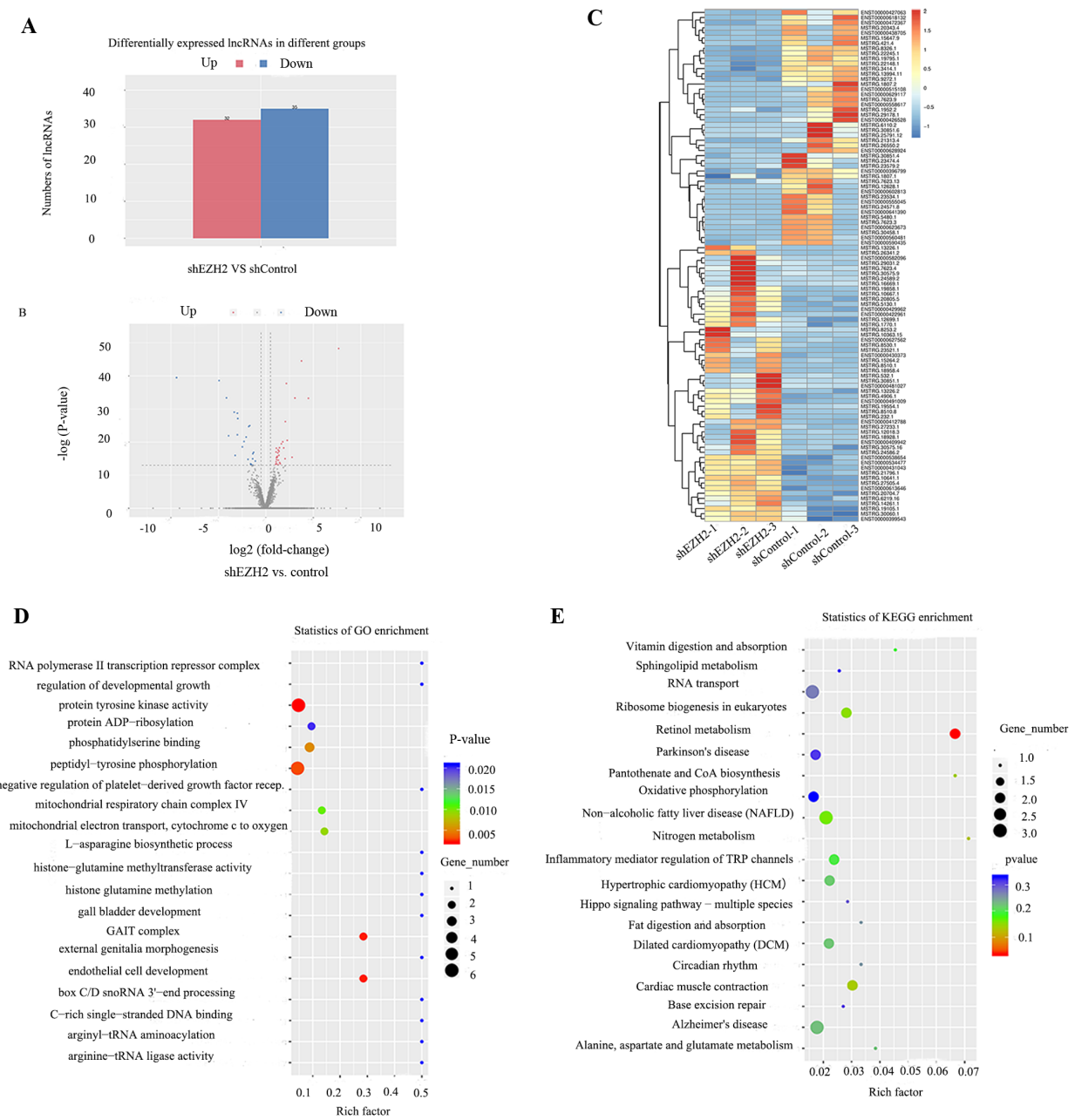

Figure 3. RNA-sequencing for differentially expressed lncRNAs. (A) Bar and (B) volcano plots and (C) heatmap of differentially expressed lncRNAs for shEZH2 vs. shControl. (D) GO and (E) Kyoto Encyclopedia of Genes and Genomes metabolic pathway enrichment analysis of peak-associated genes. lncRNA, long non-coding RNA; sh, short hairpin; EZH2, enhancer of zeste homolog 2; GO, Gene Ontology.

Table III). GO analysis demonstrated enrichment of 'nervous system development', 'chemical synaptic transmission' and 'trans-synaptic signaling' (Fig. 4C). KEGG analysis indicated that 'Rap1 signaling pathway', 'cAMP signaling pathway' and 'retrograde endocannabinoid signaling' were enriched (Fig. 4D).

Discussion

Although numerous treatments for NB currently exist, patients with NB have only 40% survival rate (2,30). A novel treatment is therefore needed to improve survival rate. EZH2 is a member of the polycomb group protein family that is upregulated in various types of cancer, including NB (31,32). Li *et al* (32) demonstrated that EZH2 knockdown significantly inhibits NB differentiation. Transcriptome sequencing has demonstrated that neurotrophic receptor tyrosine kinase 1 may be a target of EZH2. Chen *et al* (31) reported that the MYCN gene binds to the EZH2 promoter, directly promoting EZH2 expression and EZH2 inhibition of neuronal differentiation in a PRC2-dependent manner (33). Tsubota *et al* (34) demonstrated that EZH2 inhibitors significantly repress the growth of tyrosine hydroxylase-MYCN NB mice, and that MYCN and PRC2 targets are positively correlated in NB. EZH2 may therefore be considered as a novel target for NB treatment. Bate-Eya *et al* (35) demonstrated that high expression of EZH2 has a survival function independent of its methyltransferase activity in NB. Although inhibitors of EZH2 are at pre-clinical

Table II. Different lncRNAs determined by RNA-sequencing following enhancer of zeste homolog 2 knockdown.

lncRNA name	lncRNA ID	Chromosome	Regulation
MALAT1	ENST00000618132	11	Down
AL360012.1	ENST00000602813	1	Down
TTN-AS1	ENST00000629117	2	Down
AC108488.1	ENST00000422961	2	Up
EXOC3-AS1	ENST00000623673	5	Down
AC015813.1	ENST00000582096	17	Up
AC025171.2	ENST00000515108	5	Down
DHRS4-AS1	ENST00000555045	14	Down
AC027237.3	ENST00000558617	15	Down
SVIL-AS1	ENST00000427063	10	Down
SNHG15	ENST00000438705	7	Down
SNHG5	ENST00000431043	6	Up
AC125494.1	ENST00000396799	12	Down
AC079781.5	ENST00000641390	7	Down
LINC00958	ENST00000534477	11	Up
LRRC75A-AS1	ENST00000472367	17	Down
H19	ENST00000412788	11	Up
FAM212B-AS1	ENST00000430373	1	Up
AC016757.1	ENST00000409942	2	Up
AL590133.2	ENST00000560481	1	Down
THAP7-AS1	ENST00000429962	22	Up
EBLN3P	ENST00000628924	9	Down
AL139099.5	MSTRG.8510.8	14	Up
ARF4	MSTRG.21313.4	3	Down
GRAPL	MSTRG.12628.1	17	Down
AC006064.4	MSTRG.6110.2	12	Down
RBFOX2	MSTRG.20343.4	22	Down
AL139099.5	MSTRG.8510.1	14	Up
LINC00854	MSTRG.13226.1	17	Up
AC092329.3	MSTRG.15647.9	19	Down
FIRRE	MSTRG.30851.6	X	Down
AL627171.1	MSTRG.8530.1	14	Up
FAM182B	MSTRG.18928.1	20	Up
RMRP	MSTRG.29178.1	9	Down
LINC01021	MSTRG.23474.4	5	Down
AP002360.2	MSTRG.5480.1	11	Down
UBC	MSTRG.7623.9	12	Down
MST1L	MSTRG.421.4	1	Down
SNHG16	MSTRG.13994.11	17	Down
CCNG1	MSTRG.24571.8	5	Down
Z94721.1	MSTRG.26341.2	6	Up
NDUFA4	MSTRG.26550.2	7	Down
FBXL16	MSTRG.10641.1	16	Up
PANK3	MSTRG.24589.2	5	Up
LINC00854	MSTRG.13226.2	17	Up
C16orf74	MSTRG.12018.3	16	Up
MIR34AHG	MSTRG.232.1	1	Up
MAP2K3	MSTRG.12699.1	17	Up
ASXL1	MSTRG.18958.4	20	Up
TJP1	MSTRG.9272.1	15	Down
MANBAL	MSTRG.19105.1	20	Up
AL355075.4	MSTRG.8253.2	14	Up

Table II. Continued.

lncRNA name	lncRNA ID	Chromosome	Regulation
XIST	MSTRG.30575.16	X	Up
FIRRE	MSTRG.30851.1	X	Up
ZNF436-AS1	MSTRG.532.1	1	Up
RPL37	MSTRG.23579.2	5	Down
FAM111B	MSTRG.4906.1	11	Up
AC092821.3	MSTRG.6219.16	12	Up
NUp210	MSTRG.20805.5	3	Up
PARG	MSTRG.3414.1	10	Down

lncRNA, long non-coding RNA.

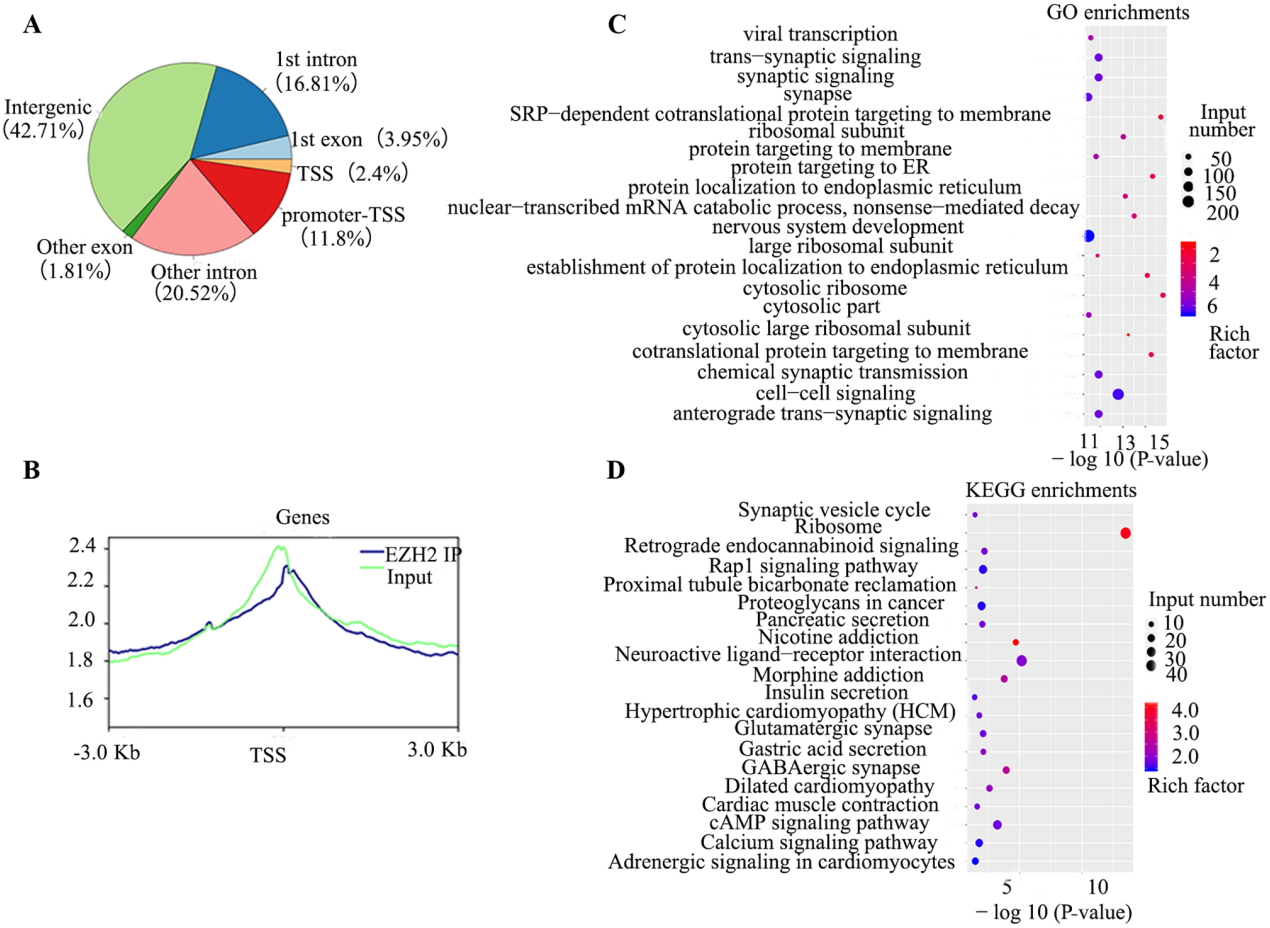

Figure 4. ChIP-seq for EZH2. (A) Peak distribution for the genomic functional area of ChIP-seq. (B) Distribution of reads at transcription start site (usually the location of transcription factor binding) for genes. (C) Gene Ontology and (D) Kyoto Encyclopedia of Genes and Genomes metabolic pathway enrichment analysis of peak-associated genes. ChIP-seq, chromatin immunoprecipitation-sequencing; EZH2, enhancer of zeste homolog 2; TSS, transcription start site.

stage in many cancers, their efficacy and underlying mechanism in NB remain unknown.

In a previous study, certain lncRNAs were demonstrated to serve key roles in NB. For example, FOXD3-antisense RNA (AS) 1 is downregulated in NB tissues and cell lines; this is an independent prognostic marker for favorable outcomes for patients with NB. FOXD3-AS1 inhibits the progression of NB via repressing poly-ADP ribose polymerase 1-mediated CCCTC-binding factor activation (36). The lncRNA pancEts-1 is upregulated and is an independent prognostic factor for unfavorable NB outcomes. In addition, pancEts-1 directly interacts with heterogeneous nuclear ribonucleoprotein K to increase its interaction with β-catenin, resulting in stabilization and transactivation of β-catenin and promotion of the growth and metastasis of NB both *in vitro* and *in vivo* (37). EZH2 is a transcriptional repressor associated with lncRNA.

Table III. Promoter of long non-coding RNA determined by chromatin immunoprecipitation-sequencing.

Gene ID	Chromosome	Start	End	Strand	Annotated_Transcript	logFC	P-value
RP11-672L10.3	18	907879	908507	-	ENST00000582554	3.129033173	1.33492×10^{-12}
KIRREL3	11	127003233	127004161	-	ENST00000533026	3.003238319	1.50761×10^{-06}
KIRREL3	11	127000973	127001187	-	ENST00000547738	3.003238319	1.50761×10^{-06}
IGF2-AS	11	2139621	2141215	+	ENST00000381361	2.877117623	1.14607×10^{-17}
AP000282.2	21	33070946	33071173	-	ENST00000454622	2.813201993	4.67603×10^{-05}
RP11-88H9.2	1	111989337	111991186	+	ENST00000438293	2.775316437	2.86341×10^{-10}
TBX5-AS1	12	114407959	114408321	+	ENST00000531202	2.734420323	9.25093×10^{-07}
MIR1-1HG	20	62549839	62550053	+	ENST00000624914	2.522145791	9.65857×10^{-10}
FLJ16779	20	63253277	63253737	+	ENST00000612722	2.510159699	1.96314×10^{-09}
RP11-92C4.6	9	98942992	98944517	-	ENST00000605631	2.391645807	1.12556×10^{-08}
RP11-672L10.2	18	904551	904765	-	ENST00000582921	2.372166725	1.71009×10^{07}
RP11-672L10.2	18	904176	904390	-	ENST00000582921	2.372166725	1.71009×10^{-07}
RP11-672L10.2	18	906549	907654	-	ENST00000581719	2.372166725	1.71009×10^{-07}
RP3-525N10.2	6	68634166	68635846	-	ENST00000604392	2.366348664	2.47756×10^{-10}
AC099754.1	3	26622451	26622769	-	ENST00000435884	2.28090657	4.94043×10^{-05}
RP11-436F23.1	4	46389763	46390468	+	ENST00000502455	2.248486391	1.13494×10^{-08}
CTC-235G5.3	5	76084156	76085290	-	ENST00000503652	2.221930293	2.35777×10^{-09}
RP11-274G22.1	X	21373658	21374071	-	ENST00000636317	2.211953324	1.02635×10^{-11}
RP11-343J3.2	10	69574708	69575542	+	ENST00000428753	2.207584122	1.94744×10^{-06}
AP002856.5	11	131252716	131253002	+	ENST00000416553	2.203360843	0.001177692
RP11-452C13.1	7	157867952	157868291	+	ENST00000608596	2.19401377	0.001695242
GPR50-AS1	X	151177247	151178372	-	ENST00000454196	2.152759945	3.44626×10^{-06}
LINC00200	10	1159259	1159473	+	ENST00000425630	2.151520464	0.000313333
RNF219-AS1	13	77918846	77919422	+	ENST00000607862	2.145410121	0.000124562
C8orf34-AS1	8	68331425	68331669	-	ENST00000512294	2.129407806	0.00016937
RP11-17E2.2	4	21948016	21948230	+	ENST00000510705	2.129407806	0.00016937
RP1-269M15.3	20	43189349	43189646	+	ENST00000611791	2.129407806	0.00016937
RP6-24A23.3	X	108735146	108736079	+	ENST00000608811	2.103500759	2.23745×10^{-05}
RP4-683L5.1	11	35418158	35420102	+	ENST00000534165	2.073937887	6.79163×10^{-10}
PTPRD-AS2	9	10612459	10613283	+	ENST00000429581	2.04619868	0.000273436
LINC01210	3	137771274	137772805	+	ENST00000478772	2.039638671	5.14222×10^{-08}
RP11-563K23.1	7	143363541	143363755	+	ENST00000609674	2.008614264	1.33265×10^{-05}
RP11-588H7.1	3	14601566	14601780	+	ENST00000635800	1.989744589	0.00057344
RP11-343P9.1	8	135456592	135457331	-	ENST00000518674	1.980487281	5.20702×10^{-06}
FGF14-AS1	13	102368126	102368468	+	ENST00000451630	1.970094904	0.004327089
CTD-2523D13.2	11	119729856	119730070	+	ENST00000533253	1.954654555	0.000134587

Table III. Continued.

Gene ID	Chromosome	Start	End	Strand	Annotated_Transcript	logFC	P-value
RP11-901H12.1	3	21227123	21227337	-	ENST00000634947	1.950333985	0.006647239
CASC16	16	52606660	52606874	-	ENST00000510238	1.943876617	0.010319298
ADGRA1-AS1	10	133088588	133089156	-	ENST00000366099	1.898488801	8.76189×10^{-06}
RP11-231C18.1	4	54331878	54332092	+	ENST00000511634	1.883283382	0.001289255
MIR519A1	19	53751934	53752148	+	ENST00000385257	1.874499442	0.025042572
MIR129-2	11	43580825	43581855	+	ENST00000362207	1.872185866	1.61125×10^{-07}
CD1E	1	158352934	158353309	+	ENST00000368167	1.847765953	0.00285251
RP11-415C15.1	4	27140713	27140939	-	ENST00000506878	1.82461652	0.001888542
RP11-21C4.1	8	64578103	64578381	-	ENST00000520834	1.797854867	1.29304×10^{-05}
AL022344.7	10	42751909	42752386	-	ENST00000568976	1.796142677	0.000430003
HAR1B	20	63102600	63103193	-	ENST00000447910	1.784741755	0.000108551
RP1-273N12.4	6	98832858	98833303	-	ENST00000635423	1.782829544	0.000111871
RP11-461O7.1	16	56190697	56191236	-	ENST00000501259	1.742859438	0.000158433
MAPT-AS1	17	45895359	45895627	-	ENST00000579599	1.733234586	9.03861×10^{-06}
RP1-90G24.10	22	32204199	32204413	+	ENST00000434942	1.705684675	0.000158433
HAR1A	20	63102059	63102459	+	ENST00000433161	1.705257532	0.000218753
LL22NC03-121E8.3	22	48141487	48141701	+	ENST00000446364	1.699601022	0.004015236
CTD-2194D22.3	5	1882806	1883957	+	ENST00000506335	1.67006809	4.45899×10^{-07}
FOXC2-AS1	16	86567608	86568108	-	ENST00000563280	1.667099473	0.000418716
MIR124-2HG	8	64376996	64377210	+	ENST00000524060	1.656091826	0.009625718
RP11-876N24.2	16	10888696	10889194	-	ENST00000572017	1.645368552	0.001847602
AC010729.1	2	5695877	5696091	+	ENST00000455579	1.634091046	0.000299766
RP11-146I2.1	6	15089927	15090141	-	ENST00000437648	1.632781249	0.005823769
CTD-2089N3.1	5	50967242	50967513	-	ENST00000510349	1.624569379	0.009038249
RP11-386B13.3	4	185051181	185051395	+	ENST00000509017	1.614500015	0.009625718
RP11-1263C18.2	4	576322	576536	+	ENST00000637674	1.611131906	0.001648005
RP11-486P11.1	7	20095996	20096210	+	ENST00000590912	1.608559926	0.014306174
CTA-125H2.2	22	25898897	25899111	-	ENST00000595102	1.601862196	0.031052599
CTA-125H2.2	22	25903547	25903761	-	ENST00000608257	1.601862196	0.031052599
RP11-140A10.3	10	132185784	132186004	-	ENST00000443922	1.597660222	0.000116767
LHX5-AS1	12	113470956	113471262	+	ENST00000551357	1.571644358	0.001181247
RP11-923I11.6	12	51816816	51817177	+	ENST00000562343	1.562378841	0.0022933
RP11-255H23.4	19	23875050	23875264	-	ENST00000599944	1.558300834	0.031052599
RP11-636O21.2	18	39841267	39841481	+	ENST00000637369	1.546964313	0.013197567
RP13-977J11.9	12	132168767	132169107	+	ENST00000619983	1.525547657	0.005463975

Table III. Continued.

Gene ID	Chromosome	Start	End	Strand	Annotated_Transcript	logFC	P-value
CTA-299D3.8	22	48547918	48548151	-	ENST00000626321	1.50297288	0.045280597
LINC01497	17	69960846	69961199	+	ENST00000455460	1.481003517	0.007180229
FGF12-AS2	3	192514512	192515287	+	ENST00000443165	1.467946667	0.004402766
AC145110.1	8	29748261	29748499	+	ENST00000517491	1.464946227	0.019169253
DOCK4-AS1	7	111808080	111808294	+	ENST00000452714	1.464946227	0.019169253
AC011513.4	19	41786996	41787210	-	ENST00000601409	1.459633143	0.006071182
RP11-347C12.11	16	30359204	30359692	+	ENST00000611264	1.442748682	0.002976471
GRM7-AS1	3	7560233	7560551	-	ENST00000427273	1.438859533	0.015604312
RP11-164C12.2	15	93423281	93423680	-	ENST00000556708	1.438859533	0.015604312
RP11-655C2.3	11	58505612	58505826	-	ENST00000527054	1.438859533	0.015604312
RP11-476M19.2	12	3367415	3367629	+	ENST00000542449	1.429070956	0.002593418
RP11-583F24.7	11	18864950	18865166	-	ENST00000524957	1.412555095	0.003778445
FGF10-AS1	5	44388123	44388744	+	ENST00000502457	1.397829443	0.000213665
LINC00342	2	95816770	95817393	-	ENST00000448494	1.39486642	0.011048418
RP11-31E13.2	10	78696881	78697101	-	ENST00000455498	1.39486642	0.011048418
CTC-490G23.2	19	43331306	43331853	-	ENST00000595748	1.393500649	0.001691433
RP11-715J22.3	16	2453190	2453657	-	ENST00000561653	1.382523434	0.009165782
CTC-293G12.1	5	100658715	100658963	-	ENST00000511592	1.377982806	0.027678904
RP11-1151B14.2	18	58415921	58416146	+	ENST00000585470	1.372986331	0.006071182
LINC00905	19	16034867	16035081	+	ENST00000589071	1.349005167	0.011418275
RP11-417J1.1	5	8524277	8524621	+	ENST00000505784	1.346034828	0.001397979
RP11-339N8.1	9	108703360	108703574	-	ENST00000415465	1.329449778	0.034844927
RP11-100E13.1	1	224615665	224615973	-	ENST00000437416	1.313540747	0.003978429
CTD-2369P2.4	19	10260054	10260664	-	ENST00000587088	1.291980197	0.008432619
RP11-120A1.1	4	21304232	21304532	+	ENST00000515680	1.290820753	0.018753813
CTC-529I10.2	17	16040460	16040674	+	ENST00000442828	1.289168246	0.019530136
RP11-404O13.1	1	158147337	158147621	-	ENST00000635685	1.289168246	0.019530136
RP11-554D14.6	12	107864072	107864415	-	ENST00000547452	1.279468004	0.006918611
CH17-125A10.2	1	144642430	144642671	-	ENST00000615763	1.278798153	0.017419713
CH17-125A10.2	1	144643049	144643263	-	ENST00000615763	1.278798153	0.017419713
RP11-308B16.2	5	12573811	12574025	-	ENST00000502209	1.271835066	0.005263785
RP5-1159O4.2	7	7553201	7553548	-	ENST00000608770	1.262358355	0.018753813
SATB1-AS1	3	18444817	18445100	+	ENST00000414198	1.243227131	0.011232888
SATB1-AS1	3	18692681	18693359	+	ENST00000425799	1.243227131	0.011232888
CTD-2278I10.1	19	17360281	17360495	+	ENST00000597592	1.242486357	0.048953034

Table III. Continued.

Gene ID	Chromosome	Start	End	Strand	Annotated_Transcript	logFC	P-value
LINC01252	12	11547257	11547497	+	ENST00000499291	1.242486357	0.048953034
LINC01194	5	12574630	12574871	+	ENST00000505196	1.210837745	0.008262948
AC002539.1	17	70074000	70074236	-	ENST00000587325	1.203691494	0.02513009
RP11-30J20.1	8	136529857	136530169	+	ENST00000524346	1.203691494	0.02513009
RP11-30J20.1	8	136536567	136536781	+	ENST00000517345	1.203691494	0.02513009
RP4-555D20.3	3	43996414	43996646	+	ENST00000605537	1.192768756	0.014908014
GFOD1-AS1	6	13486482	13486696	+	ENST00000446001	1.18462265	0.009134047
U91319.1	16	13245463	13245712	+	ENST00000571619	1.165322808	0.03830181
AC009501.4	2	63048680	63049151	-	ENST00000437346	1.160170784	0.004406531
AC000403.4	13	76887415	76887795	+	ENST00000613696	1.151662451	0.003423805
AC009404.2	2	117833865	117834191	+	ENST00000420330	1.14253746	0.044449271
CTD-3224K15.2	5	139649694	139650142	-	ENST00000514287	1.1368449	0.009213888
RP11-234B24.2	12	4719653	4719867	-	ENST00000527518	1.121955081	0.02513009
LINC00694	3	44439800	44440014	-	ENST00000636468	1.120622631	0.043957484
RP1-35C21.1	1	177350670	177350941	+	ENST00000451341	1.120622631	0.043957484
RP1-90J20.2	6	2916876	2917111	+	ENST00000437718	1.106734529	0.017533495
PABPC5-AS1	X	91435542	91435757	-	ENST00000456187	1.103269093	0.029430716
MMP25-AS1	16	3059866	3060087	-	ENST00000572574	1.099462156	0.011720469
RP11-331F9.4	9	35645503	35645717	+	ENST00000428948	1.070621547	0.038802283
RP11-307E17.8	9	94331494	94331776	+	ENST00000454869	1.069513076	0.044449271
RP11-353N14.1	17	79800162	79800376	+	ENST00000570512	1.069080411	0.004834217
RP11-297M9.1	16	9677330	9677544	-	ENST00000561538	1.060801047	0.033509944
RP11-637O11.2	3	168287466	168287707	+	ENST00000496247	1.060801047	0.033509944
RP1-253P7.4	17	17857479	17857693	+	ENST00000354746	1.060801047	0.033509944
CTB-118N6.2	5	116573419	116573633	+	ENST00000508766	1.041943716	0.018538748
CTD-2516F10.2	11	7435808	7436022	-	ENST00000530846	1.041943716	0.018538748
CASC15	6	21664562	21664824	+	ENST00000606336	1.014892605	0.030066952
RP11-410N8.3	20	32560238	32560452	+	ENST00000413983	1.008861783	0.030000331
RP11-805F19.1	18	15165032	15165460	-	ENST00000581690	0.992961131	0.043825627
RP11-452I5.2	17	74749000	74749350	-	ENST00000585285	0.958163776	0.023648425
AC009133.12	16	29821695	29821963	-	ENST00000564980	0.896472053	0.046484806
RP11-680H20.2	11	94237505	94238448	+	ENST00000506309	0.678965838	0.003627177

Numerous lncRNAs are associated with EZH2 with positive or negative correlation (38,39). Since the interacting gene product enhances the co-expressed gene, positively correlated lncRNA is a potential ligand for EZH2 or has the same transcriptional machinery as EZH2 (40). Knocking down EZH2 using small interfering RNA has previously confirmed that lncRNA is negatively correlated with EZH2 expression and is inhibited by EZH2 (41). The present study demonstrated that numerous lncRNAs were associated with EZH2. RIP-seq identified 94 lncRNAs that may bind to EZH2 directly. Among lncRNAs, Chi *et al* (42) reported that small nucleolar host gene (SNHG) 7 facilitates NB progression via the microRNA (miR)-653-5p/signal transducer and activator of transcription 2 pathway, providing a novel therapeutic target and prognostic biomarker for NB. The lncRNA family with sequence similarity 201A may affect the radiosensitivity of esophageal squamous cell cancer by regulating ataxia telangiectasia mutated (ATM) and mTOR expression via miR-101 (43). In the present study, RNA-seq demonstrated that 32 up- and 35 downregulated lncRNAs were differentially expressed in the shEZH2 group compared with the control group. Metastasis-associated lung adenocarcinoma transcript 1 (MALAT1) (44), H19 (45) and X-inactive specific transcript (XIST) (46) were some of the first reported lncRNAs associated with NB development. Koshimizu *et al* (47) demonstrated that expression level of the tumor marker MALAT1 is sensitive to cell surface receptor activation by oxytocin in an NB cell line. In addition, a six-center case-control study identified three single nucleotide polymorphisms (SNPs; rs2839698 G>A, rs3024270 C>G and rs217727 G>A) from the H19 gene in a Chinese population (700 people with NB and 1,516 controls) and investigated the effect of individual and combined SNPs on NB risk (48). Zhang *et al* (49) demonstrated that XIST downregulates the Dickkopf Wnt signaling pathway inhibitor 1 by promoting H3 histone methylation via EZH2, inhibiting proliferation, migration and invasion of NB cells and limiting tumor development. In addition, SNHG family members, SNHG5, is upregulated while SNHG15 and SNHG16 is downregulated in NB. SNHG16 is reported to facilitate proliferation, migration, invasion and autophagy of NB cells via sponging miR-542-3p and upregulating autophagy-related 5 expression levels (50). However, the involvement of these lncRNAs in NB remains unknown. Among the 138 lincRNAs identified by EZH2 ChIP-seq, cancer susceptibility 15 was identified as a tumor suppressor that can regulate numerous genes involved in neural crest development (51). GO analysis demonstrated that EZH2 participated in a number of biological processes, such as 'nervous system development', 'regulation of developmental growth' and 'histone glutamine methylation'. KEGG analysis showed that 'Hedgehog signaling pathway' was enriched in both RIP-seq and RNA-seq, indicating that the pathway may be important in EZH2-associated lincRNAs.

In conclusion, the present study demonstrated that numerous lincRNAs could directly bind to EZH2. Certain lincRNAs may regulate or be regulated by EZH2. Certain lncRNAs were associated with N6-methyladenosine and may potentially encode functional polypeptides. In addition, the difficulty of EZH2-targeted drug research may be associated with these lincRNAs. These lincRNAs may provide a novel option for EZH2-centered molecular target therapy.

Acknowledgements

Not applicable.

Funding

This study received financial support from Shanghai Key Disciplines (grant no. 2017ZZ02022), National Natural Science Foundation of China (grant nos. 81771633 and 81572324) and Science Foundation of Shanghai (grant nos. 17411960600 and 15ZR1404200).

Availability of data and materials

The datasets used during the present study are available from the corresponding author upon reasonable request.

Authors' contributions

KD, DM and MY designed the study. MY, LX and JZ collected the data and performed experiments. BL, XL and JH analyzed and interpreted the data. DM and KD were involved in critical reviewing of the manuscript. All authors read and approved the final manuscript.

Ethics approval and consent to participate

Not applicable.

Patient consent for publication

Not applicable.

Competing interests

The authors declare that they have no competing interests.

References

1. Alam MW, Boreas M, Lind DE, Cervantes-Madrid D, Umapathy G, Palmer RH and Hallberg B: Alectinib, an anaplastic lymphoma kinase inhibitor, abolishes ALK activity and growth in alk-positive neuroblastoma cells. Front Oncol 9: 579, 2019.
2. Calvo C, Storey C, Morcrette G, Akl P, Freneaux P, Pierron G, Trang H, Aerts I, Schleiermacher G, Philippe-Chomette P, *et al*: Metastatic neuroblastoma in a patient with ROHHAD: A new alert regarding the risk of aggressive malignancies in this rare condition. Pediatr Blood Cancer 66: e27906, 2019.
3. Garcia M, Rodriguez-Hernandez CJ, Mateo-Lozano S, Perez-Jaume S, Goncalves-Alves E, Lavarino C, Mora J and de Torres C: Parathyroid hormone-like hormone plays a dual role in neuroblastoma depending on PTH1R expression. Mol Oncol 13: 1959-1975, 2019.
4. Grasso S, Cangelosi D, Chapelle J, Alzona M, Centonze G, Lamolinara A, Salemme V, Angelini C, Morellato A, Saglietto A, *et al*: The SRCIN1/p140Cap adaptor protein negatively regulates the aggressiveness of neuroblastoma. Cell Death Differ 27: 790-807, 2019.
5. Bhoopathi P, Pradhan AK, Bacolod MD, Emdad L, Sarkar D, Das SK and Fisher PB: Regulation of neuroblastoma migration, invasion, and in vivo metastasis by genetic and pharmacological manipulation of MDA-9/syntenin. Oncogene 38: 6781-6793, 2019.
6. Pacenta HL and Macy ME: Entrectinib and other ALK/TRK inhibitors for the treatment of neuroblastoma. Drug Des Devel Ther 12: 3549-3561, 2018.

7. Campbell K, Shyr D, Bagatell R, Fischer M, Nakagawara A, Nieto AC, Brodeur GM, Matthay KK, London WB and DuBois SG: Comprehensive evaluation of context dependence of the prognostic impact of MYCN amplification in neuroblastoma: A report from the International Neuroblastoma Risk Group (INRG) project. Pediatr Blood Cancer 66: e27819, 2019.
8. Yu Y, Chen F, Yang Y, Jin Y, Shi J, Han S, Chu P, Lu J, Tai J, Wang S, *et al*: lncRNA SNHG16 is associated with proliferation and poor prognosis of pediatric neuroblastoma. Int J Oncol 55: 93-102, 2019.
9. Avitabile M, Lasorsa VA, Cantalupo S, Cardinale A, Cimmino F, Montella A, Capasso D, Haupt R, Amoroso L, Garaventa A, *et al*: Association of PARP1 polymorphisms with response to chemotherapy in patients with high-risk neuroblastoma. J Cell Mol Med 24: 4072-4081, 2020.
10. Ye M, Ma J, Liu B, Liu X, Ma D and Dong K: Linc01105 acts as an oncogene in the development of neuroblastoma. Oncol Rep, 2019 (Epub ahead of print).
11. Liu Z, Yang L, Zhong C and Zhou L: EZH2 regulates H2B phosphorylation and elevates colon cancer cell autophagy. J Cell Physiol 235: 1494-1503, 2019.
12. Kosalai ST, Morsy M, Papakonstantinou N, Mansouri L, Stavroyianni N, Kanduri C, Stamatopoulos K, Rosenquist R and Kanduri M: EZH2 upregulates the PI3K/AKT pathway through IGF1R and MYC in clinically aggressive chronic lymphocytic leukaemia. Epigeneticst 14: 1125-1140, 2019.
13. Pediconi N, Salerno D, Lupacchini L, Angrisani A, Peruzzi G, De Smaele E, Levrero M and Belloni L: EZH2, JMJD3, and UTX epigenetically regulate hepatic plasticity inducing retro-differentiation and proliferation of liver cells. Cell Death Dis 10: 518, 2019.
14. Kim KH and Roberts CW: Targeting EZH2 in cancer. Nat Med 22: 128-134, 2016.
15. Yan KS, Lin CY, Liao TW, Peng CM, Lee SC, Liu YJ, Chan WP and Chou RH: EZH2 in cancer progression and potential application in cancer therapy: A friend or foe? Int J Mol Sci 18: 1172, 2017.
16. Ma J, Zhang J, Weng YC and Wang JC: EZH2-mediated microRNA-139-5p regulates epithelial-mesenchymal transition and lymph node metastasis of pancreatic cancer. Mol Cells 41: 868-880, 2018.
17. Liu Q, Wang G, Li Q, Jiang W, Kim JS, Wang R, Zhu S, Wang X, Yan L, Yi Y, *et al*: Polycomb group proteins EZH2 and EED directly regulate androgen receptor in advanced prostate cancer. Int J Cancer 145: 415-426, 2019.
18. Wang C, Liu Z, Woo CW, Li Z, Wang L, Wei JS, Marquez VE, Bates SE, Jin Q, Khan J, *et al*: EZH2 mediates epigenetic silencing of neuroblastoma suppressor genes CASZ1, CLU, RUNX3, and NGFR. Cancer Res 72: 315-324, 2012.
19. Delas MJ, Jackson BT, Kovacevic T, Vangelisti S, Munera ME, Wild SA, Stork EM, Erard N, Knott S and Hannon GJ: lncRNA spehd regulates hematopoietic stem and progenitor cells and is required for multilineage differentiation. Cell Rep 27: 719-729. e6, 2019.
20. Zhong Y, Wang J, Lv W, Xu J, Mei S and Shan A: lncRNA TTN-AS1 drives invasion and migration of lung adenocarcinoma cells via modulation of miR-4677-3p/ZEB1 axis. J Cell Biochem 120: 17131-17141, 2019.
21. Cairns J, Ingle JN, Kalari KR, Shepherd LE, Kubo M, Goetz MP, Weinshilboum RM and Wang L: The lncRNA MIR2052HG regulates ERalpha levels and aromatase inhibitor resistance through LMTK3 by recruiting EGR1. Breast Cancer Res 21: 47, 2019.
22. Schmidt K, Carroll JS, Yee E, Thomas DD, Wert-Lamas L, Neier SC, Sheynkman G, Ritz J and Novina CD: The lncRNA SLNCR recruits the androgen receptor to EGR1-bound genes in melanoma and inhibits expression of tumor suppressor p21. Cell Rep 27: 2493-2507.e4, 2019.
23. Jin L, Cai Q, Wang S, Wang S, Mondal T, Wang J and Quan Z: Long noncoding RNA MEG3 regulates LATS2 by promoting the ubiquitination of EZH2 and inhibits proliferation and invasion in gallbladder cancer. Cell Death Dis 9: 1017, 2018.
24. Wang Y, Xie Y, Li L, He Y, Zheng D, Yu P, Yu L, Tang L, Wang Y and Wang Z: EZH2 RIP-seq identifies tissue-specific long non-coding RNAs. Curr Gene Ther 18: 275-285, 2018.
25. Su M, Xiao Y, Tang J, Wu J, Ma J, Tian B, Zhou Y, Wang H, Yang D, Liao QJ and Wang W: Role of lncRNA and EZH2 interaction/regulatory network in lung cancer. J Cancer 9: 4156-4165, 2018.
26. Kim B: Western blot techniques. Methods Mol Biol 1606: 133-139, 2017.
27. Gagliardi M and Matarazzo MR: RIP: RNA immunoprecipitation. Methods Mol Biol 1480: 73-86, 2016.
28. Xia W, Hu J, Ma J, Huang J, Jing T, Deng L, Zhang J, Jiang N, Ma D and Ma Z: Mutations in TOP2B cause autosomal-dominant hereditary hearing loss via inhibition of the PI3K-Akt signalling pathway. Febs Lett 593: 2008-2018, 2019.
29. Kong L, Tan L, Lv R, Shi Z, Xiong L, Wu F, Rabidou K, Smith M, He C, Zhang L, *et al*: A primary role of TET proteins in establishment and maintenance of De Novo bivalency at CpG islands. Nucleic Acids Res 44: 8682-8692, 2016.
30. Ozcelik D and Pezacki JP: Small molecule inhibition of protein disulfide isomerase in neuroblastoma cells induces oxidative stress response and apoptosis pathways. Acs Chem Neurosci 10: 4068-4075, 2019.
31. Chen L, Alexe G, Dharia NV, Ross L, Iniguez AB, Conway AS, Wang EJ, Veschi V, Lam N, Qi J, *et al*: CRISPR-Cas9 screen reveals a MYCN-amplified neuroblastoma dependency on EZH2. J Clin Invest 128: 446-462, 2018.
32. Li Z, Takenobu H, Setyawati AN, Akita N, Haruta M, Satoh S, Shinno Y, Chikaraishi K, Mukae K, Akter J, *et al*: EZH2 regulates neuroblastoma cell differentiation via NTRK1 promoter epigenetic modifications. Oncogene 37: 2714-2727, 2018.
33. Bellamy J, Szemes M, Melegh Z, Dallosso A, Kollareddy M, Catchpoole D and Malik K: Increased efficacy of histone methyltransferase G9a inhibitors against MYCN-amplified neuroblastoma. Front Oncol 10: 818, 2020.
34. Tsubota S, Kishida S, Shimamura T, Ohira M, Yamashita S, Cao D, Kiyonari S, Ushijima T and Kadomatsu K: PRC2-mediated transcriptomic alterations at the embryonic stage govern tumorigenesis and clinical outcome in MYCN-driven neuroblastoma. Cancer Res 77: 5259-5271, 2017.
35. Bate-Eya LT, Gierman HJ, Ebus ME, Koster J, Caron HN, Versteeg R, Dolman M and Molenaar JJ: Enhancer of zeste homologue 2 plays an important role in neuroblastoma cell survival independent of its histone methyltransferase activity. Eur J Cancer 75: 63-72, 2017.
36. Zhao X, Li D, Huang D, Song H, Mei H, Fang E, Wang X, Yang F, Zheng L, Huang K and Tong Q: Risk-associated long noncoding RNA FOXD3-AS1 inhibits neuroblastoma progression by repressing PARP1-mediated activation of CTCF. Mol Ther 26: 755-773, 2018.
37. Li D, Wang X, Mei H, Fang E, Ye L, Song H, Yang F, Li H, Huang K, Zheng L and Tong Q: Long noncoding RNA pancEts-1 promotes neuroblastoma progression through hnRNPK-mediated β-catenin stabilization. Cancer Res 78: 1169-1183, 2018.
38. Wu Q, Xiang S, Ma J, Hui P, Wang T, Meng W, Shi M and Wang Y: Long non-coding RNA CASC15 regulates gastric cancer cell proliferation, migration and epithelial mesenchymal transition by targeting CDKN1A and ZEB1. Mol Oncol 12: 799-813, 2018.
39. Sanli I, Lalevee S, Cammisa M, Perrin A, Rage F, Lleres D, Riccio A, Bertrand E and Feil R: Meg3 non-coding RNA expression controls imprinting by preventing transcriptional upregulation in cis. Cell Rep 23: 337-348, 2018.
40. Wang M, Guo C, Wang L, Luo G, Huang C, Li Y, Liu D, Zeng F, Jiang G and Xiao X: Long noncoding RNA GAS5 promotes bladder cancer cells apoptosis through inhibiting EZH2 transcription. Cell Death Dis 9: 238, 2018.
41. Zheng W and Yu A: EZH2-mediated suppression of lncRNA-LET promotes cell apoptosis and inhibits the proliferation of post-burn skin fibroblasts. Int J Mol Med 41: 1949-1957, 2018.
42. Chi R, Chen X, Liu M, Zhang H, Li F, Fan X, Wang W and Lu H: Role of SNHG7-miR-653-5p-STAT2 feedback loop in regulating neuroblastoma progression. J Cell Physiol 234: 13403-13412, 2019.
43. Chen M, Liu P, Chen Y, Chen Z, Shen M, Liu X, Li X, Li A, Lin Y, Yang R, *et al*: Long noncoding RNA FAM201A mediates the radiosensitivity of esophageal squamous cell cancer by regulating ATM and mTOR expression via miR-101. Front Genet 9: 611, 2018.
44. Tripathi V, Ellis JD, Shen Z, Song DY, Pan Q, Watt AT, Freier SM, Bennett CF, Sharma A, Bubulya PA, *et al*: The nuclear-retained noncoding RNA MALAT1 regulates alternative splicing by modulating SR splicing factor phosphorylation. Mol Cell 39: 925-938, 2010.
45. Dugimont T, Curgy JJ, Wernert N, Delobelle A, Raes MB, Joubel A, Stehelin D and Coll J: The H19 gene is expressed within both epithelial and stromal components of human invasive adenocarcinomas. Biol Cell 85: 117-124, 1995.
46. Kelley RL and Kuroda MI: Noncoding RNA genes in dosage compensation and imprinting. Cell 103: 9-12, 2000.

47. Koshimizu TA, Fujiwara Y, Sakai N, Shibata K and Tsuchiya H: Oxytocin stimulates expression of a noncoding RNA tumor marker in a human neuroblastoma cell line. Life Sci 86: 455-460, 2010.
48. Li Y, Zhuo ZJ, Zhou H, Liu J, Zhang J, Cheng J, Zhou H, Li S, Li M, He J and Xiao Y: H19 gene polymorphisms and neuroblastoma susceptibility in Chinese children: A six-center case-control study. J Cancer 10: 6358-6363, 2019.
49. Zhang J, Li WY, Yang Y, Yan LZ, Zhang SY, He J and Wang JX: LncRNA XIST facilitates cell growth, migration and invasion via modulating H3 histone methylation of DKK1 in neuroblastoma. Cell Cycle 18: 1882-1892, 2019.
50. Wen Y, Gong X, Dong Y and Tang C: Long non coding RNA SNHG16 facilitates proliferation, migration, invasion and autophagy of neuroblastoma cells via sponging miR-542-3p and upregulating ATG5 expression. Onco Targets Ther 13: 263-275, 2020.
51. Russell MR, Penikis A, Oldridge DA, Alvarez-Dominguez JR, McDaniel L, Diamond M, Padovan O, Raman P, Li Y, Wei JS, *et al*: CASC15-S is a tumor suppressor lncRNA at the 6p22 neuroblastoma susceptibility locus. Cancer Res 75: 3155-3166, 2015.